

The Atmospheric Imaging Radar – Ubiquitous Radar

Feng Nai^{1,2}, Robert Palmer^{1,3}, Sebastian Torres^{1,4,5}, James Kurdzo^{1,3} and David Bodine^{1,3}

¹Advanced Radar Research Center, University of Oklahoma, Norman, OK, U.S.A.

²School of Electrical and Computer Engineering, University of Oklahoma, Norman, OK, U.S.A.

³School of Meteorology, University of Oklahoma, Norman, OK, U.S.A.

⁴Cooperative Institute for Mesoscale Meteorological Studies, University of Oklahoma, Norman, OK, U.S.A.

⁵NOAA/OAR National Severe Storms Laboratory, Norman, OK, U.S.A.

Atmospheric Imaging Radar

The Atmospheric Imaging Radar (AIR) is a X-band mobile weather radar developed at the Advanced Radar Research Center (ARRC) at the University of Oklahoma (OU). It is unique in that it applies imaging technology to gather precipitation data, as opposed to clear air data collected with imaging predecessors. By transmitting over a large field-of-view (FOV) and receiving on 36 independent receive subarrays, simultaneous RHI sampling can be achieved with high temporal resolution through digital beamforming (DBF). Because of the rapid update time, the AIR is uniquely equipped to observe rapidly evolving tornados and other severe storms.



The AIR deployed to observe a tornado near Carmen, OK on April 14, 2012. These are the first simultaneous cross-section measurements through a tornado.

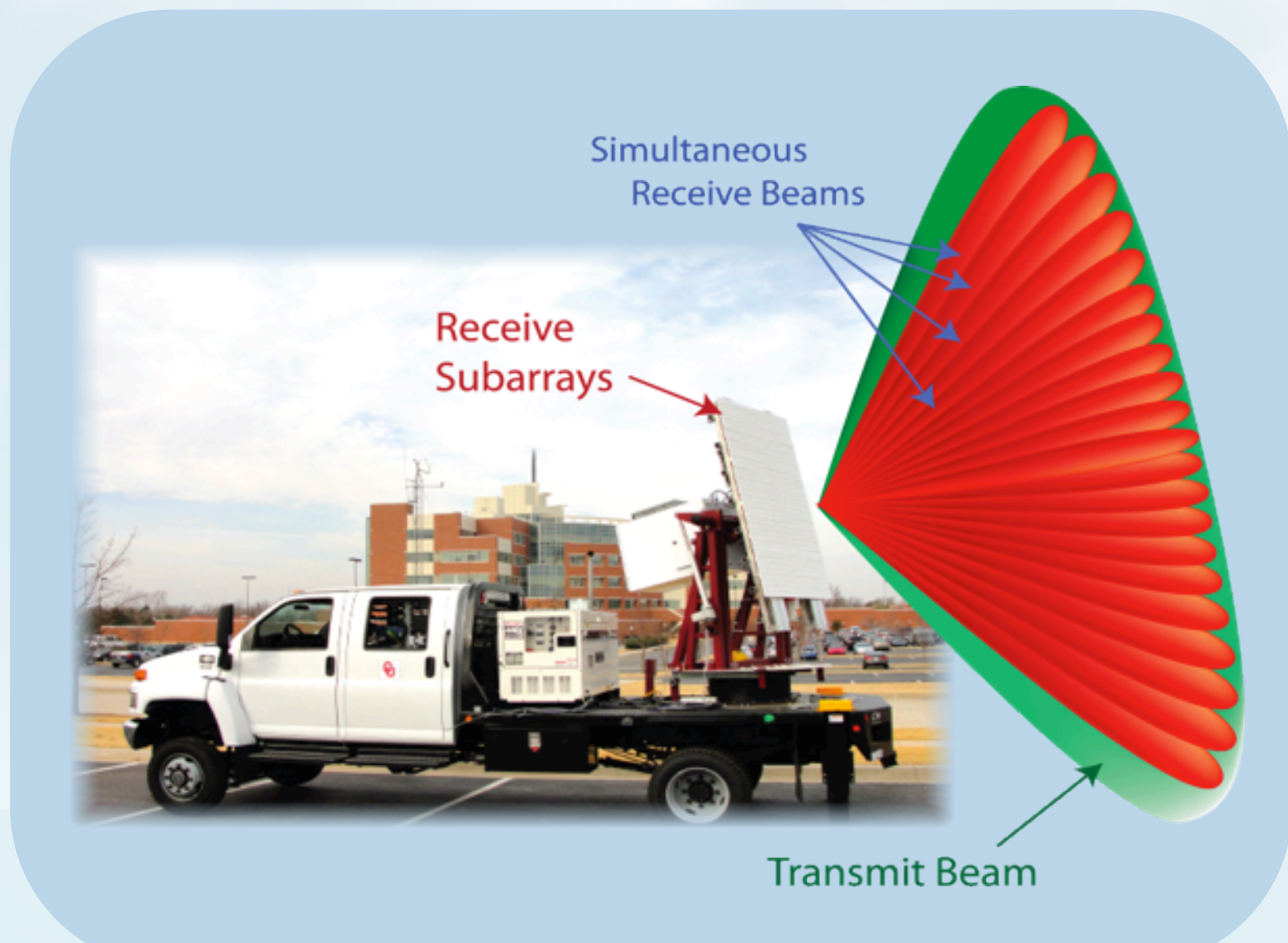
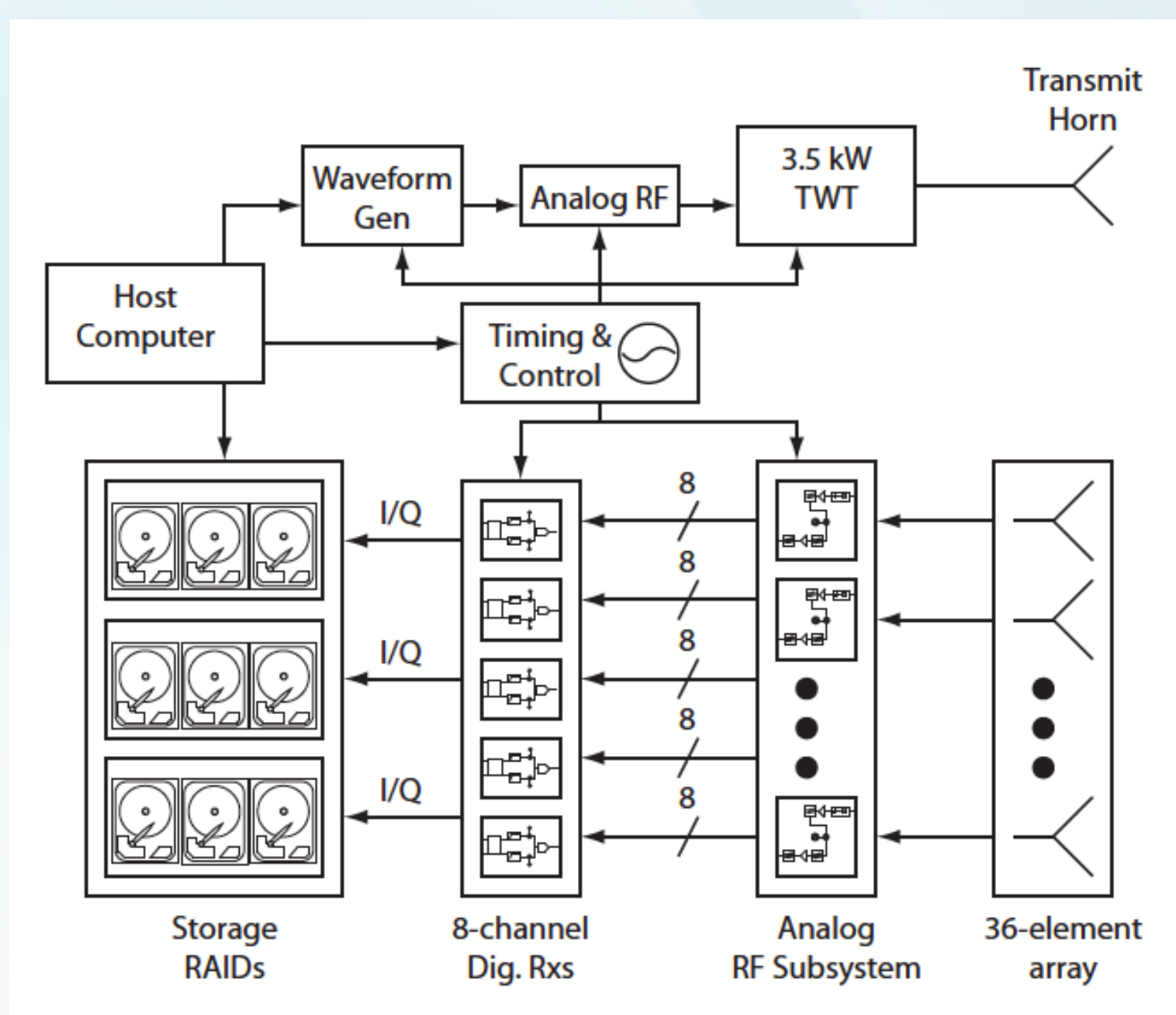


Photo of the AIR along with illustration of the wide transmit beam and digitally formed simultaneous receive beams.



Block diagram of the AIR. I/Q data from each receiver is stored and can be summed with designed weights to form beams.

System Overview

AIR uses a 3.5 kW TWT amplifier, which is capable of producing an 8 μ s pulse at a 2500 Hz PRF, to generate the output transmit signal. To achieve the desired sensitivity and range resolution, pulse compression techniques will be utilized with flexible waveforms that are generated by an arbitrary waveform generator. A slotted waveguide array is used to transmit a 1° x 20° FOV beam.

Each of the 36 receive subarrays is itself an array of patch antennas and has an individual down-conversion unit mounted on the back of the casing. The approximate subarray spacing for AIR is 1.8 λ , which results in grating lobes located around $\pm 33^\circ$ from broadside. Since the grating lobes are outside of the FOV of the transmit beam, it does not pose a significant problem unless the main beam is steered to the edges of the FOV. Other technical specifications for the air are shown below.

Sensitivity	<10 dBZ @10 km 0 SNR	Polarization
Range Resolution	30 m (pulse compression)	Size
Array		
Beamwidth	1° x 1°	Rotation R
Number of Subarrays	36	Controller
Aperture	1.2 x 1.8 m	Gear Ratio
Configurable Array	Linear	
Transmit Horn		
Beamwidth	1° x 20°	Type
Gain	28.5 dBi	ADC
Size	1.5 x 0.12 m	Sampling R
Slotted Waveguide Array		

135

Digital Beamforming

By coherently combining the output of the 36 independent receive subarrays, the AIR can accurately estimate the amplitude and phase of a signal for a particular direction. The equation that describes the beamforming process is:

$$\mathbf{y}(t) = \mathbf{w}^* \mathbf{x}(t) \quad (1)$$

where $\mathbf{x}(t)$ is a vector of received signals from M subarrays, \mathbf{w} is a selected weighting vector that controls the direction of the formed beam, and $\mathbf{y}(t)$ is the complex voltage signal corresponding to that direction. \mathbf{w} can be chosen independent of \mathbf{x} , as done in Fourier method, or be determined adaptively based on the received data, as done in Capon's method and robust Capon method.

\mathbf{w}_{FB} for Fourier beamforming for a given θ is given by

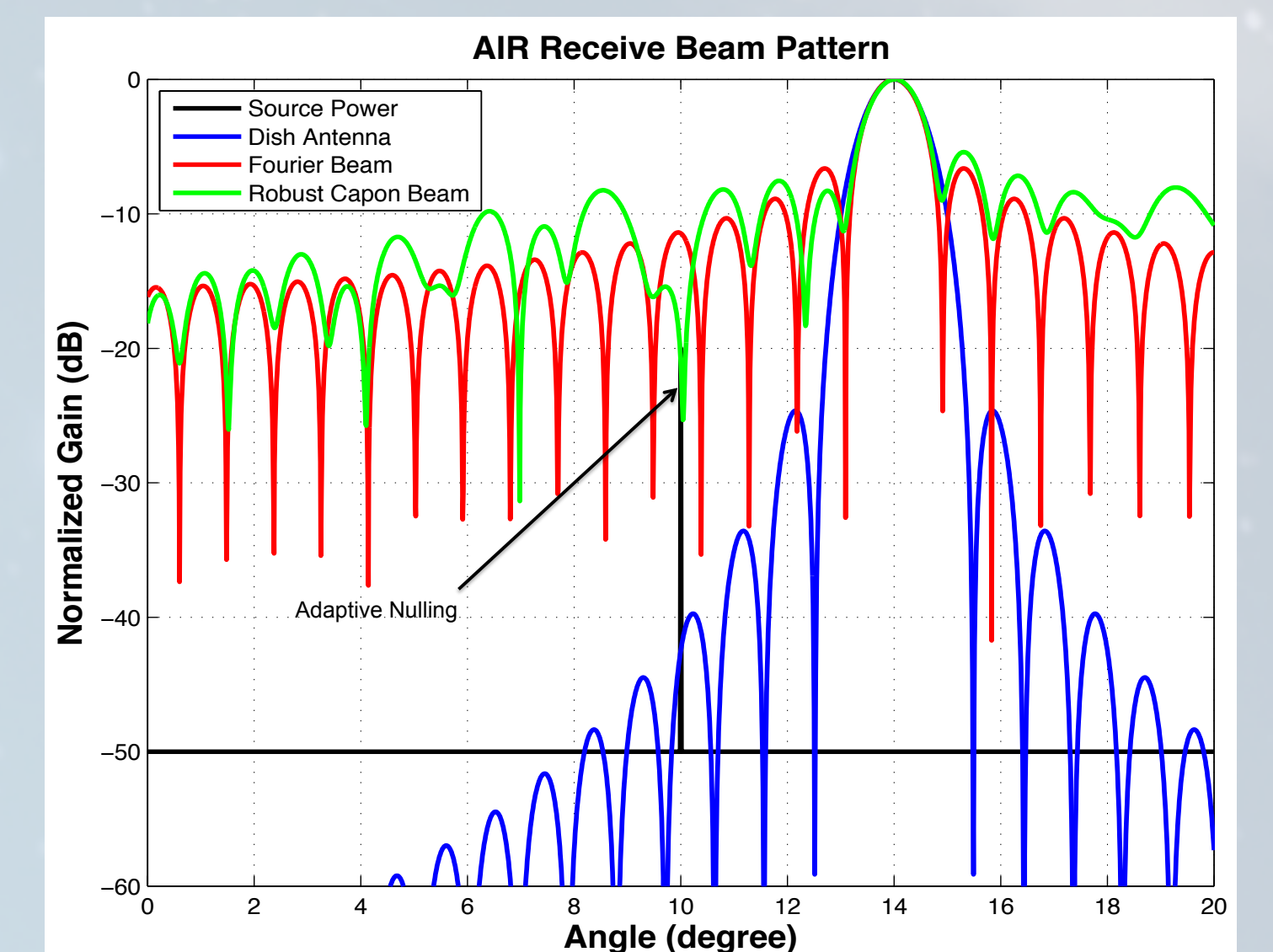
$$\mathbf{w}_{FB}(\theta) = \frac{1}{M} \begin{bmatrix} 1 & e^{-jkd \sin \theta} & \dots & e^{-j(M-1)kd \sin \theta} \end{bmatrix}^T \quad (2)$$

where k is the wave number, d is the spacing between subarrays, and θ is the desired beam direction measured from broadside.

Adaptive beamforming methods alter the weighting vector based on received data to minimize the impact of interfering signals in the sidelobes. One such method is Capon's method, which seeks to minimize the output power while maintain unity gain in the desired direction. \mathbf{w}_{CP} for Capon method is given by

$$\mathbf{w}_{CP}(\theta) = M \frac{\mathbf{R}_{xx}^{-1} \mathbf{w}_{FB}(\theta)}{\mathbf{w}_{FB}^*(\theta) \mathbf{R}_{xx}^{-1} \mathbf{w}_{FB}(\theta)} \quad (3)$$

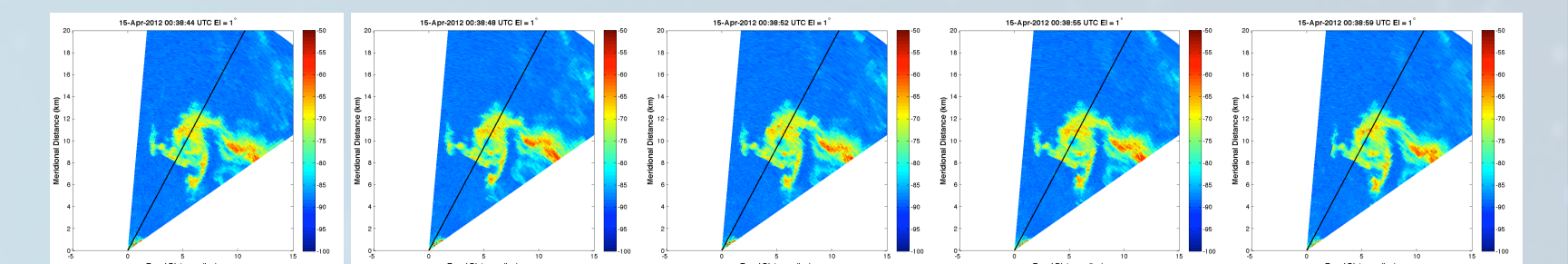
where $\mathbf{R}_{xx} = E\{\mathbf{x}(t)\mathbf{x}^*(t)\}$ is the spatial autocovariance matrix at lag 0. Capon's method can usually provide higher angular resolution than Fourier method, but its performance suffers from uncertain knowledge of element positions in the array. Such errors could result in the signal of interest being attenuated by Capon's method because it is offset from the angle where the beam is constrained to have unity gain. As a result, a more robust version of Capon's method was developed to handle uncertainties in element positions. The figure below demonstrates the capability of robust Capon method to adaptively reject interference signals.



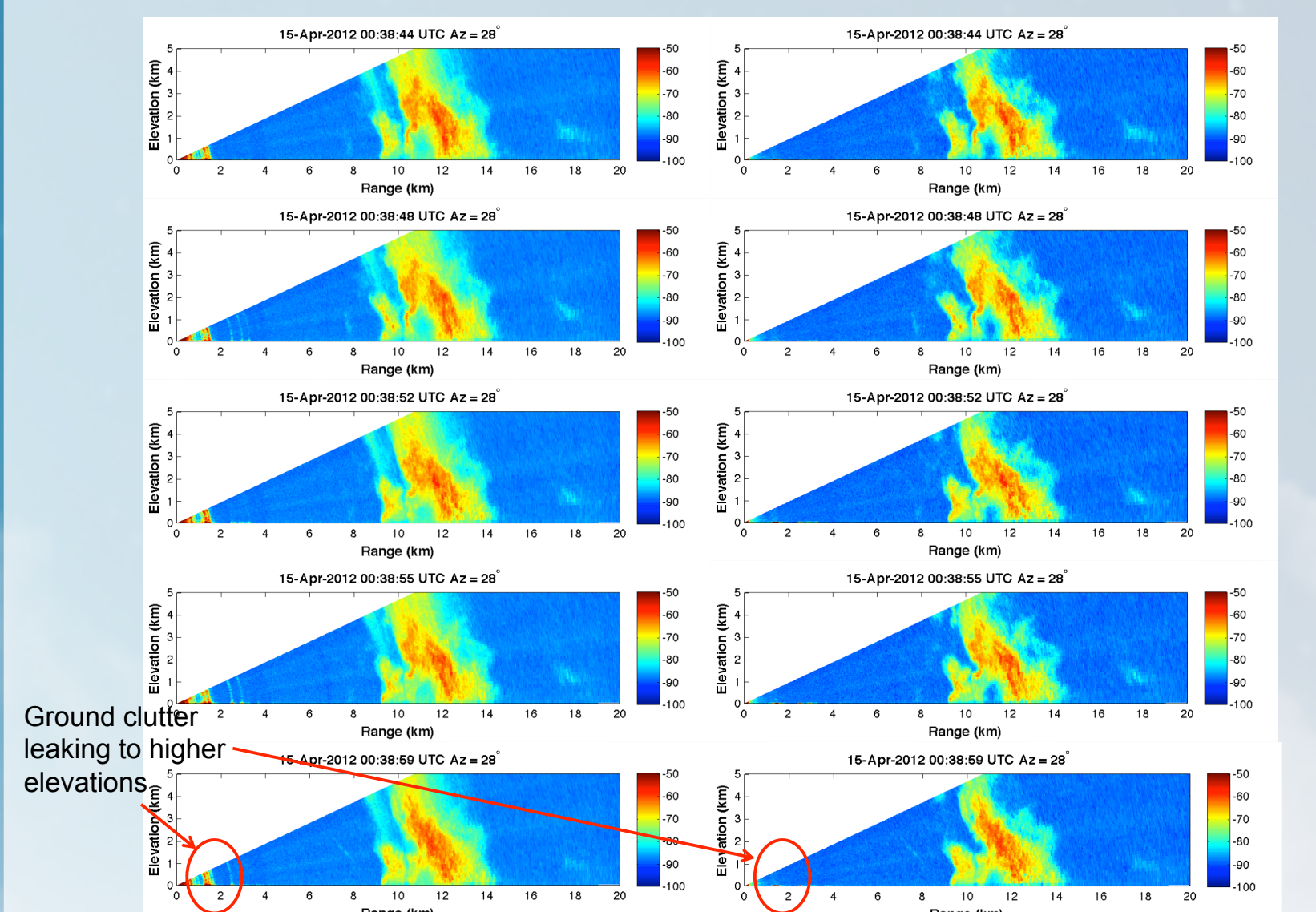
Receive beam pattern comparison between a dish antenna with the same aperture size as the overall array for air (blue), Fourier beam (red), and robust Capon beam (green). The beams are pointed at 14° and an interfering signal is present at 10° as indicated by the black curve. Notice that the robust Capon beam has placed a null at the angle of the interfering signal.

Weather Observations

The AIR was deployed on April 14, 2012 near Carmen, OK to collect the first simultaneous cross-section measurements through a tornado. The update time is approximately 3.5 seconds for the sector scan.



PPI plots of 5 consecutive sector scans at 1° elevation showing the tornado's evolution.



RHI plots of 5 consecutive sector scans at 28° azimuth angle showing the tornado's evolution. Notice ground clutter leakage to higher elevation angle in the Fourier method (left) is not present in the robust Capon method (right).



This work is partially supported by the National Severe Storms Laboratory (NOAA/NSSL) under cooperative agreement NA08OAR4320904. The authors would like to give special thanks to Brad Isom and John Meier for all their help and suggestions for the project.

